

An Improved Adaptive Sidelobe Blanker

Francesco Bandiera and Danilo Orlando

Abstract—We propose a two stage detector consisting of a Subspace Detector (SD) followed by the Whitenes Adaptive Beamformer Orthogonal Rejection Test (W-ABORT). The performance analysis shows that it possesses the Constant False Alarm Rate property with respect to the unknown covariance matrix of the noise and that it guarantees a wider range of directivity values with respect to previously proposed two stage detectors. The probability of false alarm and the probability of detection (for both matched and mismatched signals) have been evaluated in closed form.

Index Terms—Adaptive Radar Detection, Adaptive Sidelobe Blanker, Constant False Alarm Rate, Mismatched Signals.

I. INTRODUCTION

IN the last decades several papers have addressed adaptive radar detection of targets embedded in Gaussian or non-Gaussian disturbance. Most of these papers follow the lead of the seminal paper by Kelly [1], where the Generalized Likelihood Ratio Test (GLRT) is used to conceive an adaptive decision scheme capable of detecting coherent pulse trains in presence of Gaussian disturbance with unknown spectral properties. In [2] it is shown that an ad hoc detector, based on the two-step GLRT-based design procedure, can also achieve better detection performance than Kelly's detector; such an ad hoc detector will be referred to in the following as Adaptive Matched Filter (AMF). Detection of point-like targets in non-Gaussian noise has been dealt with in [3, and references therein].

The case of point-like targets assumed to belong to a known subspace of the observables has been addressed in [4], [5]. In addition, several detection algorithms for point-like or extended targets embedded in Gaussian disturbance are encompassed as special cases of the amazingly general framework and derivation described in [6].

All of the above papers assume that returns from the target can be modeled in terms of (a linear combination of) deterministic signals known up to multiplicative, possibly complex, constants, taking into account both target and channel effects. Moreover, those detectors rely on the assumption that a set of secondary data, namely returns free of signals components, but sharing the spectral properties of the noise in the data under test, is available. Such secondary data are used to come up with fully-adaptive detection schemes.

However, previously-cited detectors have been designed without taking into account the possible presence of mismatched signals. As a matter of fact, the actual signal backscattered from a target (or target's scattering centers) can be

different from the nominal one. A mismatched signal may arise due to several reasons as, for example, [7], [8]

- coherent scattering from a direction different to that in which the radar system is steered (sidelobe target);
- imperfect modeling of the mainlobe target by the nominal steering vector, where the mismatch may be due to multipath propagation, array calibration uncertainties, beamforming errors, etc.

Thus, it might be important to trade detection performance of mainlobe targets for rejection capabilities of sidelobe ones. In order to face with this dilemma, the Adaptive Beamformer Orthogonal Rejection Test (ABORT) detector was introduced in [7]. The idea of ABORT is to modify the null hypothesis, which usually states that the vector under test contains noise only, so that it possibly contains a vector which, in some way, is orthogonal to the assumed target's signature. Doing so, if a signal with actual steering vector different from the nominal one is present, the detector will be less inclined to declare a detection, as the null hypothesis will be more plausible. For instance, if a sidelobe target is present, the ABORT detector will exhibit less false alarms than detectors which are rather sensitive to mismatched signals, such that the AMF. As customary, it is assumed that a set of secondary data is available at the receiver. The directivity of such detector is in between that of the Kelly's detector (which, in turn, is more directive than the AMF) and the one of the Adaptive Coherence Estimator (ACE) [3], [4].

However, in the original ABORT formulation, the fictitious signal under the null hypothesis was assumed to be orthogonal to the nominal one, in the *quasi-whitened* space, i.e., after whitening by the sample covariance matrix of the training samples. In [11], such an assumption was modified to address the adaptive detection of distributed targets embedded in homogeneous disturbance, by resorting to the GLRT assuming that the useful and the fictitious signals are orthogonal in the *whitened* space, i.e., after whitening with the true covariance matrix. This seemingly minor modification led to significant differences compared to ABORT and, more particularly, to an enhanced rejection of sidelobe signals. Furthermore, in [11] it is shown that such detector, referred to in the following as Whitenes ABORT (W-ABORT), may become even more selective than the ACE.

On the other hand, increased robustness can be achieved by resorting to the tools of subspace detection, namely assuming that the target belongs to a known subspace of the observables, or also constraining the possible useful signals to belong to a proper cone with axis the whitened nominal steering vector [9], [10]. Moreover, extending such a cone idea by modeling the null hypothesis as the complement of a cone to the entire space of the observables leads to a family of detectors capable of

F. Bandiera and D. Orlando are with the Dipartimento di Ingegneria dell'Innovazione, Università del Salento, Via Monteroni, 73100 Lecce, Italy. Phone: +39 0832 297207. Fax: +39 0832 325362. E-Mail: [francesco.bandiera, danilo.orlando]@unile.it.

trading detection performance of mainlobe targets for rejection capabilities of sidelobe ones.

Another class of detectors which combines the statistics of the Kelly's detector and of the AMF has been proposed by Kalson [12]: the detector statistic depends on a design parameter $\alpha \in [0, 1]$ that allows to obtain receiver operating characteristics, actually the Probability of Detection (P_d) vs signal-to-noise ratio, in between that of the Kelly's detector and the one of the AMF. Moreover, a way to combine the ABORT rationale with the subspace idea has been dealt with in [8] as a possible means to retain an acceptable detection loss for slightly mismatched mainlobe targets.

Unfortunately, though, it seems difficult to find a decision scheme capable of providing at the same time good capabilities to reject sidelobe targets and high power in case of slightly mismatched mainlobe targets. In order to face with this problem, the so-called two-stage detectors have been proposed; such schemes are formed by cascading two detectors (usually with opposite behaviors): the overall one declares the presence of a target in the data under test only when data test cells survive both detection thresholdings. A rather famous two-stage detector is the Adaptive Sidelobe Blanker (ASB). The ASB has been proposed as a means for mitigating the high number of false alarms of the AMF in the presence of undernulled interference [13]. It can be seen as the cascade of the AMF and the ACE. Remarkably, it can adjust directivity by proper selection of the two thresholds in order to trade good rejection capabilities of sidelobe targets for acceptable loss of matched signals [14]. Richmond has also provided closed-form expressions for the P_d and the Probability of False Alarm (P_{fa}) of the ASB and demonstrated that in homogeneous environment and with matched signals it has higher or commensurate P_d , for a given P_{fa} , than both the AMF and the ACE and an overall performance that is commensurate with Kelly's detector [16]. A further two-stage detector, consisting of the cascade of the AMF and the Kelly's detector, has been proposed as a computationally efficient implementation of the latter [14]. More recently, the Subspace-based ASB (S-ASB) has been proposed in order to increase the robustness of the composite detector [15]. Specifically, the S-ASB is obtained cascading a subspace GLRT-based detector (referred to in the following as subspace detector (SD)) and the ACE; the performance assessment has shown that such solution can increase the robustness of the composite detector while retaining the same selectivity.

Based upon the experience of [15], herein we propose a two-stage detector aimed at increasing also the selectivity of the S-ASB, i.e., the capability to reject mismatched signals. This is accomplished by cascading the SD and the W-ABORT. The performance assessment, carried out in closed form, seems to confirm that its directivity varies in a wider range than that of the S-ASB, when for both decision schemes we constrain the maximum loss with respect to the Kelly's detector for matched signals, given P_{fa} and P_d .

The reminder of the paper is organized as follows: next section is devoted to the problem formulation and to the description of the proposed detector while Section III contains its performance assessment; to this end, we derive closed-

form expressions of P_{fa} and P_d (for matched and mismatched signals). In Section IV we report some illustrative examples in which we compare the performance of the proposed detector with those of the S-ASB and ASB. Finally, some concluding remarks are given in Section V.

II. PROBLEM FORMULATION

Assume that a linear array formed by N_a antennas senses the cell under test and that each antenna collects N_t samples. Denote by $\mathbf{z} \in \mathbb{C}^{N \times 1}$ the N -dimensional column vector, with $N = N_a N_t$, containing returns from the cell under test. We want to test whether or not \mathbf{z} contains useful target echoes. As customary, we assume that a set of K secondary data, $\mathbf{z}_k \in \mathbb{C}^{N \times 1}$, $k = 1, \dots, K$, $K \geq N$, namely data free of signal components but sharing the same statistical properties of the noise in the cell under test, is available.

The detection problem can be re-cast as

$$\begin{cases} H_0 : \begin{cases} \mathbf{z} = \mathbf{n}, \\ \mathbf{z}_k = \mathbf{n}_k, \quad k = 1, \dots, K, \end{cases} \\ H_1 : \begin{cases} \mathbf{z} = \alpha \mathbf{p} + \mathbf{n}, \\ \mathbf{z}_k = \mathbf{n}_k, \quad k = 1, \dots, K, \end{cases} \end{cases}$$

where

- \mathbf{n} and the $\mathbf{n}_k \in \mathbb{C}^{N \times 1}$, $k = 1, \dots, K$, are independent and identically distributed complex normal random vectors with zero-mean and unknown covariance matrix \mathbf{R} , i.e., $\mathbf{n}, \mathbf{n}_k \sim \mathcal{CN}_N(\mathbf{0}, \mathbf{R})$, $k = 1, \dots, K$, with $\mathbf{R} \in \mathbb{C}^{N \times N}$ a positive definite covariance matrix;
- $\mathbf{p} \in \mathbb{C}^{N \times 1}$ is the direction of the (possible) target echo, possibly different from that of the nominal steering vector $\mathbf{v} \in \mathbb{C}^{N \times 1}$ due to imperfect modeling of the mainlobe target;
- $\alpha \in \mathbb{C}$ is an unknown deterministic factor which accounts for both target and channel effects.

In the following we propose and assess a two-stage detector obtained by cascading the SD [5], [6], whose statistic is given by

$$t_{\text{SD}} = \frac{\mathbf{z}^\dagger \mathbf{S}^{-1} \mathbf{H} (\mathbf{H}^\dagger \mathbf{S}^{-1} \mathbf{H})^{-1} \mathbf{H}^\dagger \mathbf{S}^{-1} \mathbf{z}}{1 + \mathbf{z}^\dagger \mathbf{S}^{-1} \mathbf{z}}, \quad (1)$$

and the W-ABORT, whose statistic is given by [11]

$$t_{\text{WA}} = \frac{(1 + \mathbf{z}^\dagger \mathbf{S}^{-1} \mathbf{z})^{-1}}{\left[\frac{|\mathbf{z}^\dagger \mathbf{S}^{-1} \mathbf{v}|^2}{(1 + \mathbf{z}^\dagger \mathbf{S}^{-1} \mathbf{z})(\mathbf{v}^\dagger \mathbf{S}^{-1} \mathbf{v})} - 1 \right]^2}, \quad (2)$$

where

- \dagger denotes conjugate transpose;
- $\mathbf{S} \in \mathbb{C}^{N \times N}$ is K times the sample covariance matrix of the secondary data, i.e., $\mathbf{S} = \mathbf{Z} \mathbf{Z}^\dagger$ with $\mathbf{Z} = [\mathbf{z}_1 \dots \mathbf{z}_K] \in \mathbb{C}^{N \times K}$;
- $\mathbf{H} \in \mathbb{C}^{N \times r}$ is a full-column-rank matrix (and, hence, $r > 1$ is the rank of \mathbf{H}). Obviously, the choice of \mathbf{H} will impact on the performance of the overall detector; in order to guarantee reliable detection of mismatched mainlobe targets, it seems reasonable to set $\mathbf{H} = [\mathbf{v} \mathbf{v}_1]$ namely to consider a signal subspace spanned by the

nominal steering vector and an additional one slightly mismatched with respect to \mathbf{v} .

Notice that

$$t_k = \frac{|\mathbf{z}^\dagger \mathbf{S}^{-1} \mathbf{v}|^2}{(1 + \mathbf{z}^\dagger \mathbf{S}^{-1} \mathbf{z})(\mathbf{v}^\dagger \mathbf{S}^{-1} \mathbf{v})}$$

is the well-known decision statistic of the Kelly's detector [1].

Summarizing, the operation of the newly-proposed detector, referred to in the following as Whitened ABORT and Subspace-based ASB (WAS-ASB), can be pictorially described as follows

$$\begin{array}{ccc} t_{\text{SD}} > \eta & \xrightarrow{> \eta} & t_{\text{WA}} > \xi & \xrightarrow{> \xi} & H_1 \\ & \downarrow < \eta & & \downarrow < \xi & \\ & H_0 & & H_0 & \end{array},$$

where η and ξ form the threshold pair to be set in order to guarantee the overall desired P_{fa} .

III. PERFORMANCE ASSESSMENT

In this section, we derive closed-form expressions for the P_d and P_{fa} of the WAS-ASB; to this end, we replace t_{SD} with the equivalent decision statistic $\tilde{t}_{\text{SD}} = 1/(1 - t_{\text{SD}})$. Based upon the procedure presented in [15], it is possible to show that \tilde{t}_{SD} and t_{WA} admit the following stochastic representations

$$\begin{aligned} \tilde{t}_{\text{SD}} &= (\tilde{t}_k + 1)(1 + c), \\ t_{\text{WA}} &= \frac{(\tilde{t}_k + 1)}{(1 + b)(1 + c)}, \end{aligned}$$

where b and c are random variables whose distributions depend on the hypothesis in force and $\tilde{t}_k = t_k/(1 - t_k)$. Furthermore, the explicit expressions of b and c , as functions of data, are omitted for the sake of brevity.

Under the H_0 hypothesis,

- \tilde{t}_k , given b and c , is ruled by a complex central F-distribution with $1, K - N + 1$ degrees of freedom [1] (for a definition of complex normal related statistics see also Appendix A of [16]);
- b is a complex central F-distributed random variable (rv) with $N - r, K - N + r + 1$ degrees of freedom, i.e., $b \sim \mathcal{CF}_{N-r, K-N+r+1}$ (see Appendix II of [15]);
- $c \sim \mathcal{CF}_{r-1, K-N+2}$ (see Appendix II of [15]);
- b and c are statistically independent rv's (see Appendix II of [15]).

Now, the P_{fa} of the two-stage detector can be expressed as in equation (3), shown at the top of the next page, where $\tilde{\eta} = 1/(1 - \eta)$, $p_b(\cdot)$ is the probability density function (pdf) of the rv $b \sim \mathcal{CF}_{N-r, K-N+r+1}$, $p_c(\cdot)$ is the pdf of the rv $c \sim \mathcal{CF}_{r-1, K-N+2}$, and $\mathcal{P}_0(\cdot)$ is the cumulative distribution function (CDF) of the rv \tilde{t}_k , given b and c (and under H_0), i.e., the CDF of a rv ruled by the $\mathcal{CF}_{1, K-N+1}$ distribution. Finally, observe that the P_{fa} does not depend on \mathbf{R} and, hence, this implies that the proposed WAS-ASB possesses the generalized CFAR property.

On the other hand, under the H_1 hypothesis, we assume a misalignment between the actual steering vector \mathbf{p} and the nominal one \mathbf{v} , i.e., $\mathbf{v} \neq \mathbf{p}$. In this case, rv's b and c depend on the mismatch angle (referred to in the sequel as θ) between

the actual steering vector and the nominal one in the whitened observation space. For this reason, in the following, we will denote these rv's by b_θ and c_θ . Due to the useful signal components, the distributions of \tilde{t}_k , b_θ , and c_θ change, more precisely

- \tilde{t}_k , given b_θ and c_θ , is ruled by a complex noncentral F-distribution with $1, K - N + 1$ degrees of freedom and non-centrality parameter

$$\delta_\theta^2(\text{SNR}, b, c) = \frac{\text{SNR} \cos^2 \theta}{(1 + b)(1 + c)},$$

where

$$\text{SNR} = |\alpha|^2 \mathbf{p}^\dagger \mathbf{M}^{-1} \mathbf{p}$$

is the total available signal-to-noise ratio and

$$\cos^2 \theta = \frac{|\mathbf{v}^\dagger \mathbf{R}^{-1} \mathbf{p}|^2}{(\mathbf{v}^\dagger \mathbf{R}^{-1} \mathbf{v})(\mathbf{p}^\dagger \mathbf{R}^{-1} \mathbf{p})};$$

- b_θ is ruled by a complex noncentral F-distribution with $N - r, K - N + r + 1$ degrees of freedom and non-centrality parameter

$$\delta_{b_\theta}^2 = \text{SNR} \sin^2 \theta \|\mathbf{h}_{B_1}\|^2,$$

i.e., $b_\theta \sim \mathcal{CF}_{\delta_{b_\theta}}(N - r, K - N + r + 1)$;

- given b_θ , $c_\theta \sim \mathcal{CF}_{\delta_{c_\theta}}(r - 1, K - N + 2)$, with

$$\delta_{c_\theta}^2 = \frac{\text{SNR} \sin^2 \theta \|\mathbf{h}_{B_0}\|^2}{1 + b};$$

finally, $\mathbf{h}_{B_0} \in \mathbb{C}^{(r-1) \times 1}$ and $\mathbf{h}_{B_1} \in \mathbb{C}^{(N-r) \times 1}$ are such that $\|\mathbf{h}_{B_0}\|^2 + \|\mathbf{h}_{B_1}\|^2 = 1$ (see also [17]).

Thus, following the same line of reasoning used for the derivation of the P_{fa} , it is easy to see that the P_d is given by equation (4), shown at the top of the next page, where $\mathcal{P}_{\delta_\theta}(\cdot)$ is the CDF of the rv \tilde{t}_k , given b_θ and c_θ (and under H_1), i.e., the CDF of a rv ruled by the $\mathcal{CF}_{1, K-N+1}(\delta_\theta)$ distribution, $p_{b_\theta}(\cdot)$ is the pdf of a rv ruled by the $\mathcal{CF}_{N-r, K-N+r+1}(\delta_{b_\theta})$, and $p_{c_\theta|b_\theta}(\cdot|\cdot)$ is the pdf of a rv ruled by the $\mathcal{CF}_{r-1, K-N+2}(\delta_{c_\theta})$. Note also that the dependence of P_d on the signal parameters is entirely confined to the defined signal-to-noise ratio SNR.

In the case of a perfect match between \mathbf{v} and \mathbf{p} , i.e., $\theta = 0$, δ_{b_θ} and δ_{c_θ} are equal to zero, thus rv's c_θ and b_θ obey to the complex central F-distributions with $N - r, K - N + r + 1$ and $r - 1, K - N + 2$ degrees of freedom, respectively. On the other hand, \tilde{t}_k is still subject to the noncentral complex F-distribution with $1, K - N + 1$ degrees of freedom, but the non-centrality parameter is given by

$$\delta_0(\text{SNR}, b_0, c_0) = \frac{\text{SNR}}{(1 + b_0)(1 + c_0)}.$$

IV. ILLUSTRATIVE EXAMPLES AND DISCUSSION

In this section we present some numerical examples to show the effectiveness of the WAS-ASB, also in comparison to the S-ASB and the ASB. All curves have been obtained by means of numerical integration techniques based upon the above formulas for P_{fa} and P_d .

In all examples, the noise is modeled as an exponentially-correlated complex normal vector with one-lag correlation

$$\begin{aligned}
P_{fa}(\eta, \xi) &= \mathbf{P}[t_{SD} > \eta, t_{WA} > \xi; H_0] = \mathbf{P}[\tilde{t}_{SD} > \tilde{\eta}, t_{WA} > \xi; H_0] \\
&= \mathbf{P}\left[\left(\tilde{t}_k + 1\right)(1+c) > \tilde{\eta}, \frac{\tilde{t}_k + 1}{(1+c)(1+b)} > \xi; H_0\right] \\
&= 1 - \mathbf{P}\left[\tilde{t}_k \leq \max\left(\frac{\tilde{\eta}}{1+c} - 1, \xi(1+b)(1+c) - 1\right); H_0\right] \\
&= 1 - \int_0^{+\infty} \int_0^{+\infty} \mathbf{P}\left[\tilde{t}_k \leq \max\left(\frac{\tilde{\eta}}{1+\gamma} - 1, \xi(1+\beta)(1+\gamma) - 1\right) \mid b = \beta, c = \gamma; H_0\right] \\
&\quad \times p_b(\beta) p_c(\gamma) d\beta d\gamma \\
&= 1 - \int_0^{+\infty} \int_0^{+\infty} \mathcal{P}_0\left(\max\left(\frac{\tilde{\eta}}{1+\gamma} - 1, \xi(1+\beta)(1+\gamma) - 1\right)\right) p_b(\beta) p_c(\gamma) d\beta d\gamma, \tag{3}
\end{aligned}$$

$$\begin{aligned}
P_d(\text{SNR}, \eta, \xi, \theta) &= \mathbf{P}[t_{SD} > \eta, t_{WA} > \xi; H_1] = \mathbf{P}[\tilde{t}_{SD} > \tilde{\eta}, t_{WA} > \xi; H_1] \\
&= \mathbf{P}\left[(1+c_\theta)(\tilde{t}_k + 1) > \tilde{\eta}, \frac{\tilde{t}_k + 1}{(1+b_\theta)(1+c_\theta)} > \xi; H_1\right] \\
&= 1 - \int_0^{+\infty} \int_0^{+\infty} \mathcal{P}_{\delta_\theta}(\text{SNR}, \beta, \gamma) \left(\max\left(\frac{\tilde{\eta}}{1+\gamma} - 1, \xi(1+\beta)(1+\gamma) - 1\right)\right) \\
&\quad \times p_{b_\theta c_\theta}(\beta, \gamma) d\beta d\gamma \\
&= 1 - \int_0^{+\infty} \int_0^{+\infty} \mathcal{P}_{\delta_\theta}(\text{SNR}, \beta, \gamma) \left(\max\left(\frac{\tilde{\eta}}{1+\gamma} - 1, \xi(1+\beta)(1+\gamma) - 1\right)\right) \\
&\quad \times p_{c_\theta|b_\theta}(\gamma|b_\theta = \beta) p_{b_\theta}(\beta) d\beta d\gamma, \tag{4}
\end{aligned}$$

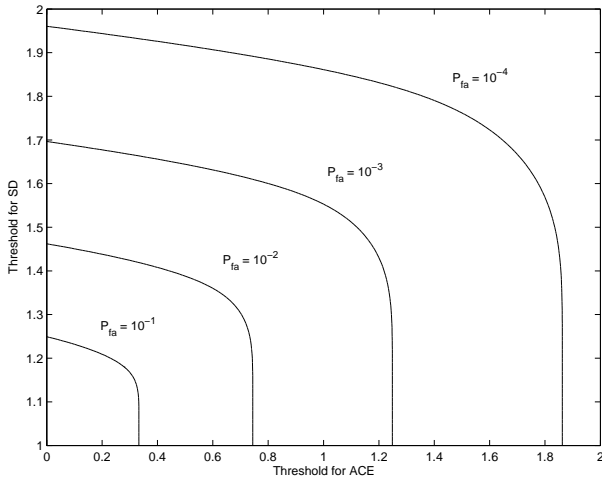


Fig. 1. Contours of constant P_{fa} for S-ASB with $N = 16$, $K_S = 32$, and $r = 2$.

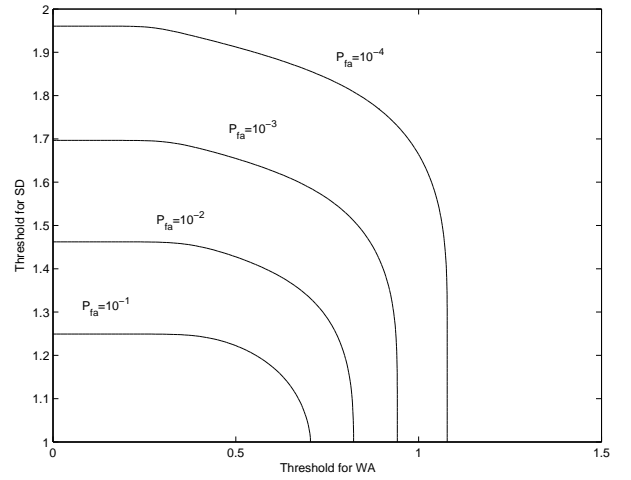


Fig. 2. Contours of constant P_{fa} for WAS-ASB with $N = 16$, $K_S = 32$, and $r = 2$.

coefficient r , namely the (i, j) -th element of the covariance matrix \mathbf{R} is given by $r^{|i-j|}$, $i, j = 1, \dots, N$, with $r = 0.95$. The probability of false alarm is set to 10^{-4} . Moreover, we set $N_t = 1$, $N_a = N = 16$, $K_s = 32$, $r = 2$, and choose $\mathbf{v} = \mathbf{s}(0)$ and $\mathbf{v}_1 = \mathbf{s}(\pi/90)$ with

$$\mathbf{s}(\phi) = \frac{1}{\sqrt{N}} [1 \ e^{j\frac{2\pi d}{\lambda} \sin \phi} \ \dots \ e^{j(N-1)\frac{2\pi d}{\lambda} \sin \phi}]^T,$$

where d is the interelement spacing, λ is the radar operating wavelength, and T denotes transpose. Moreover, we will

denote by ϕ_T the azimuthal angle of the impinging useful target echo, i.e., $\mathbf{p} = \mathbf{s}(\phi_T)$.

First, note that the P_{fa} of two-stage detectors depends on the two thresholds; as a consequence, there exist infinite threshold pairs that guarantee the same value of P_{fa} . Figs. 1 and 2 show the contour plots for the S-ASB and the WAS-ASB, respectively, corresponding to different values of P_{fa} , as functions of the thresholds pairs. It can be seen that the two detectors exhibit slightly different behaviors when the threshold of the second stage tends to zero; specifically, it

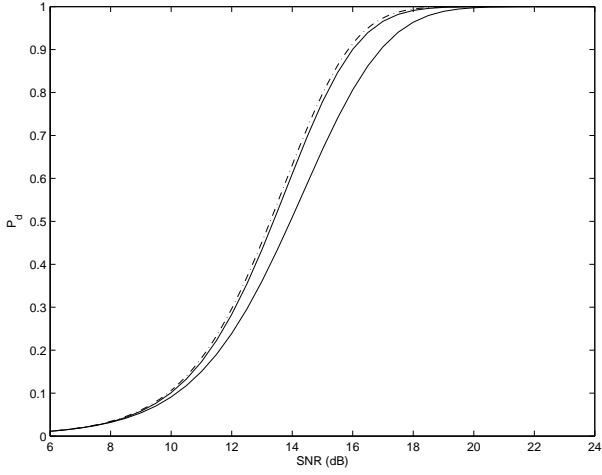


Fig. 3. P_d vs SNR for the S-ASB (solid lines) and the Kelly's detector (dash-dotted line) with $N = 16$, $K_S = 32$, and $r = 2$.

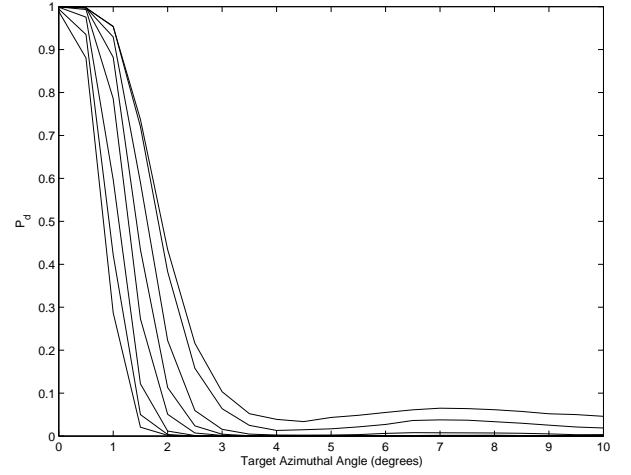


Fig. 5. P_d vs target azimuthal angle for the ASB with $N = 16$, $K_S = 32$, $r = 2$, and SNR = 19 dB.

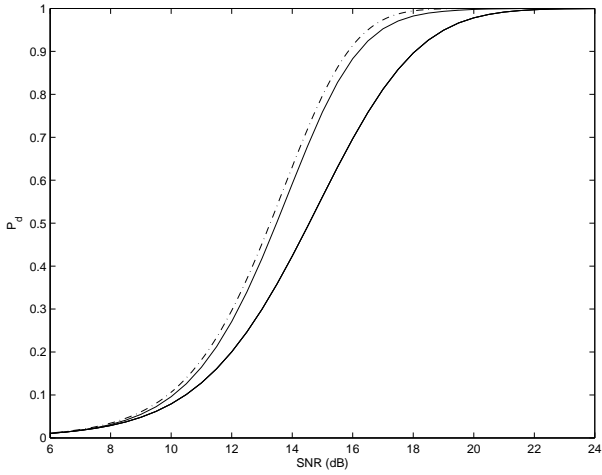


Fig. 4. P_d vs SNR for the WAS-ASB (solid lines) and the Kelly's detector (dash-dotted line) with $N = 16$, $K_S = 32$, and $r = 2$.

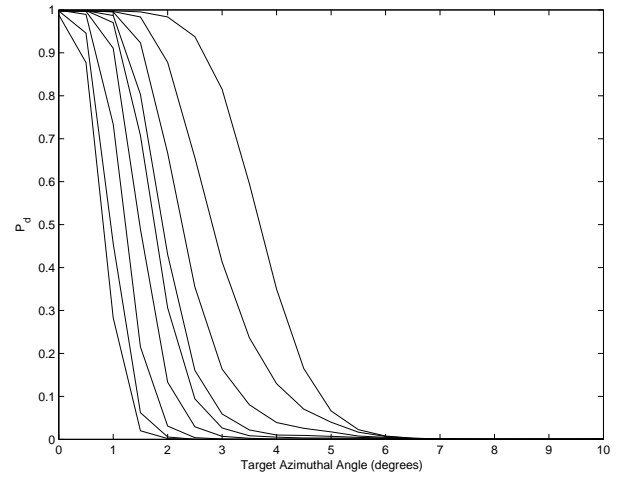


Fig. 6. P_d vs target azimuthal angle for the S-ASB with $N = 16$, $K_S = 32$, $r = 2$, and SNR = 19 dB.

is seen from Fig. 2 that, for a preassigned P_{fa} , the threshold of the SD does not change for values of the threshold of the W-ABORT ranging from 0 to 0.2.

In Figs. 3 and 4 we plot the P_d vs SNR for the S-ASB and WAS-ASB, respectively, as they compare to Kelly's detector [1], for the case of a matched mainlobe target; in these figures we show two curves for both the S-ASB and the WAS-ASB: such curves correspond to the limiting behaviors of the two detectors for threshold settings which guarantee $P_{fa} = 10^{-4}$. Fig. 3 shows that the maximum loss of the S-ASB with respect to the Kelly's detector is less than (about) 1.2 dB (at $P_d = 0.9$); such a maximum loss increases to (about) 2 dB in Fig. 4 for the WAS-ASB. In Figs. 5-7 we plot P_d vs ϕ_T (measured in degrees) for the ASB, the S-ASB, and the WAS-ASB, respectively; for all the three detectors plotted curves refer to those threshold pairs which ensure a maximum loss with respect to the Kelly's detector less than 1 dB at $P_d = 0.9$ and $P_{fa} = 10^{-4}$. Observe from Figs. 5 and 6 that the S-ASB ensures better robustness with respect to the ASB, due to the

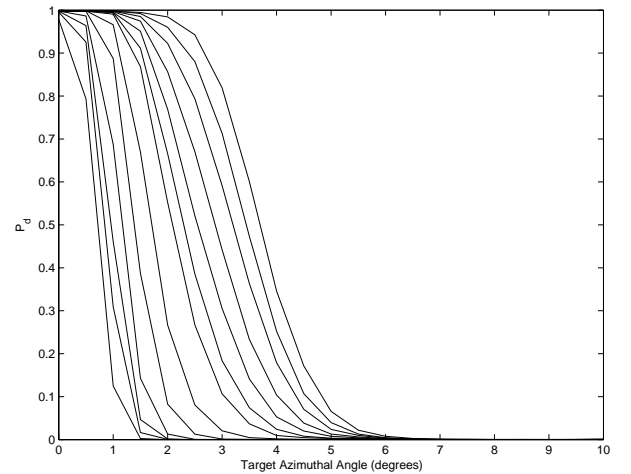


Fig. 7. P_d vs target azimuthal angle for the WAS-ASB with $N = 16$, $K_S = 32$, $r = 2$, and SNR = 19 dB.

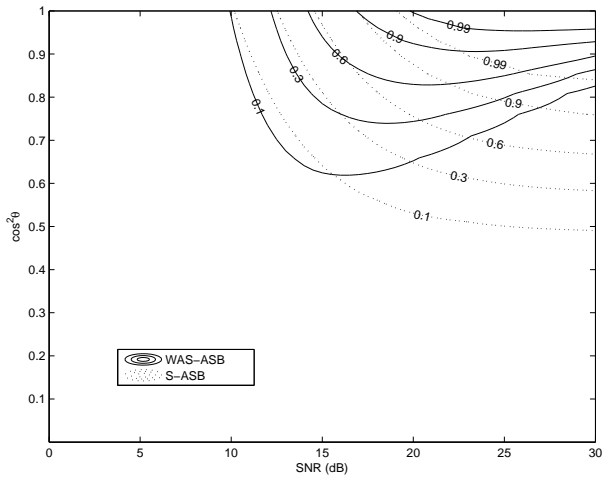


Fig. 8. Contours of constant P_d for WAS-ASB and S-ASB with $N = 16$, $K_S = 32$, $r = 2$, and threshold pairs corresponding to the most selective case.

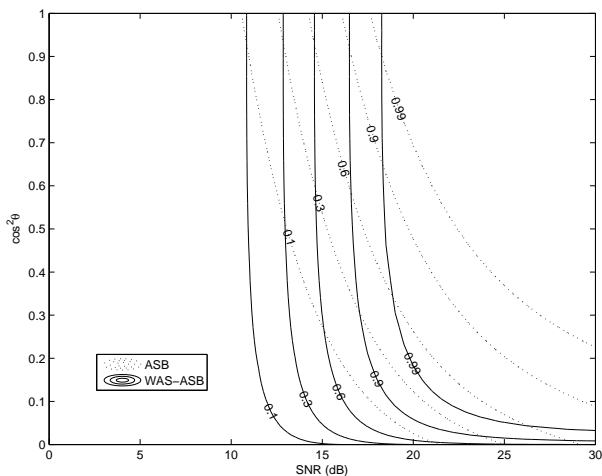


Fig. 9. Contours of constant P_d for WAS-ASB and S-ASB with $N = 16$, $K_S = 32$, $r = 2$, and threshold pairs corresponding to the most robust case.

first stage (the SD), which is less sensitive than the AMF to mismatched signals. However, S-ASB and ASB exhibits the same capability to reject sidelobe targets, according to the fact that the second stage (the ACE) is the same. As it can be seen from Fig. 7, instead, the WAS-ASB can guarantee the same robustness of the S-ASB, but better rejection capabilities, due to the fact that the second stage has been replaced by the W-ABORT.

In order to gain a deeper insight into the behavior of such two stage detectors, in Figs. 8 and 9, we plot contours of constant P_d , as functions of SNR and $\cos^2 \theta$; as for the curves of Figs. 5 and 7, thresholds settings are such that the loss from Kelly's detector is less than 1 dB for the perfectly matched case. More precisely, in Fig. 8 we evaluate the capability to reject unwanted sidelobe targets and, to this end, we compare the WAS-ASB and the S-ASB (which differ in the second stage); as it can be seen, the WAS-ASB is superior to the S-ASB in rejecting mismatched signals. In Fig. 9 we analyze

the robustness with respect to mismatched signals and compare the WAS-ASB and the ASB (which differ in the first stage); the plots show again that the WAS-ASB can be made less sensitive to steering mismatches.

V. CONCLUSION

We have proposed a two stage detector consisting of a GLRT-based subspace detector followed by the W-ABORT. The performance analysis has been conducted analytically for both matched and mismatched signals. It has shown that the proposed detector possesses the CFAR property with respect to the unknown covariance matrix of the noise and that it guarantees a wider range of directivity values with respect to the ASB and the S-ASB, so emerging as a viable means to trade detection performance of mainlobe targets for rejection capabilities of sidelobe ones.

REFERENCES

- [1] E. J. Kelly, "An Adaptive Detection Algorithm," *IEEE Trans. on Aerospace and Electronic Systems*, Vol. 22, No. 2, pp. 115-127, March 1986.
- [2] F. C. Robey, D. L. Fuhrman, E. J. Kelly, and R. Nitzberg, "A CFAR Adaptive Matched Filter Detector," *IEEE Trans. on Aerospace and Electronic Systems*, Vol. 29, No. 1, pp. 208-216, January 1992.
- [3] E. Conte, M. Lops, and G. Ricci, "Asymptotically Optimum Radar Detection in Compound Gaussian Noise," *IEEE Trans. on Aerospace and Electronic Systems*, Vol. 31, No. 2, pp. 617-625, April 1995.
- [4] L. L. Scharf and T. McWhorter, "Adaptive matched subspace detectors and adaptive coherence estimators," in *Proceedings of the 30th Asilomar Conference Signals Systems Computers*, Pacific Grove, CA, November 3-6 1996, pp. 1114-1117.
- [5] S. Kraut, L. L. Scharf, and L. T. McWhorter, "Adaptive Subspace Detectors," *IEEE Trans. on Signal Processing*, Vol. 49, No. 1, pp. 1-16, January 2001.
- [6] E. J. Kelly and K. Forsythe, "Adaptive Detection and Parameter Estimation for Multidimensional Signal Models," Lincoln Lab, MIT, Lexington, Tech. Rep. No. 848, April 19, 1989.
- [7] N. B. Pulsone and C. M. Rader, "Adaptive Beamformer Orthogonal Rejection Test," *IEEE Trans. on Signal Processing*, Vol. 49, No. 3, pp. 521-529, March 2001.
- [8] G. A. Fabrizio, A. Farina, and M. D. Turley, "Spatial Adaptive Subspace Detection in OTH Radar," *IEEE Trans. on Aerospace and Electronic Systems*, Vol. 39, No. 4, pp. 1407-1427, October 2003.
- [9] A. De Maio, "Robust Adaptive Radar Detection in the Presence of Steering Vector Mismatches," *IEEE Trans. on Aerospace and Electronic Systems*, Vol. 41, No. 4, pp. 1322-1337, October 2005.
- [10] F. Bandiera, A. De Maio, and G. Ricci, "Adaptive CFAR Radar Detection with Conic Rejection," *IEEE Trans. on Signal Processing*, in print.
- [11] F. Bandiera, O. Besson, and G. Ricci, "An ABORT-like detector with improved mismatched signals rejection capabilities," *IEEE Transactions Signal Processing*, 2007, under revision.
- [12] S. Z. Kalson, "An Adaptive Array Detector with Mismatched Signal Rejection," *IEEE Trans. on Aerospace and Electronic Systems*, Vol. 28, No. 1, pp. 195-207, January 1992.
- [13] C. D. Richmond, "Performance of a Class of Adaptive Detection Algorithms in Nonhomogeneous Environments," *IEEE Trans. on Signal Processing*, Vol. 48, No. 5, pp. 1248-1262, May 2000.
- [14] N. B. Pulsone and M. A. Zatman, "A Computationally Efficient Two-Step Implementation of the GLRT," *IEEE Trans. on Signal Processing*, Vol. 48, No. 3, pp. 609-616, March 2000.
- [15] F. Bandiera, D. Orlando, and G. Ricci, "A Subspace-based Adaptive Sidelobe Blanker," *IEEE Trans. on Signal Processing*, 2007, submitted for publication.
- [16] C. D. Richmond, "Performance of the Adaptive Sidelobe Blanker Detection Algorithm in Homogeneous Environments," *IEEE Trans. on Signal Processing*, Vol. 48, No. 5, pp. 1235-1247, May 2000.
- [17] E. J. Kelly, "Performance of an adaptive detection algorithm; rejection of unwanted signals," *IEEE Transactions Aerospace Electronic Systems*, vol. 25, no. 2, pp. 122-133, April 1989.